tubes and from a ballistic range. All measurements were made by calorimetric gauges mounted at the stagnation point of hemisphere cylinders. The test gas was air. The shock tube data are by Rose and Stark,[10] Rose and Stankevics,[11] and Horton and Babineaux.[12] Rose and Stankevics carried out a specific analysis to determine both the thermochemical state of air and the effects of catalycity of the surface of the calorimeter. Their conclusion was that air was frozen in the boundary layer and the wall catalytic effect was negligible. The analysis by Rose and Stark relied on the comparison with the results by the Fay–Riddell correlation formulas. Their conclusion was that air was in equilibrium. Horton and Babineaux did not perform such an analysis. The ballistic range data are by Yee et al.[13] The heat flux was measured by launching from a light gas gun small models flying through air. The measurements were made at an ambient temperature of 300 K and at an ambient pressure of 0.1 atm. According to the opinion of Yee et al., for these conditions the stagnation density is so high (approximately atmospheric) that air in the shock layer is in equilibrium.

The comparison of the normalized heat fluxes is shown in Fig. 3. The match of the present results with the ones by H2NS is excellent in the whole range of enthalpy potential. The match with the experimental data is pretty good up to the enthalpy difference of 14 MJ/kg for each state of the gas. At low enthalpy levels, in fact, the dissociation is not remarkable, and thus it is not really necessary to specify the state of the gas. The present results show a reasonable good agreement with the data by Rose and Stankevics. The agreement with the data by Horton and Babineaux is also good. This agreement indicates that the test gas considered by Horton and Babineaux should be in nonequilibrium and the wall of the calorimeter should be fully catalytic.

IV. Conclusions

Fay and Riddell's classical solution concerning the stagnation point heat transfer in high-speed flow was reexamined. The approximations used in the Fay–Riddell work were identified, and some of them are removed in the present procedure.

Numerical results by the present procedure were validated with existing ground test data and Navier–Stokes results. Good agreement between the present results and experimental data is noted. Therefore, the improved Fay–Riddell procedure can be a ready-to-use tool for researchers in hypersonic wind-tunnel experiments. It is particularly useful to assess the wall catalycity effects of the test models.

More general models for the transport coefficients, e.g., the Yun–Mason model, and the variability of the vibrational temperature in the boundary layer can be easily included in the present procedure.

References

[1]Fay, J. A., and Riddell, F. R., "Theory of Stagnation Point Heat Transfer in Dissociated Air," *Journal of the Aeronautical Sciences*, Vol. 25, No. 2, 1958, pp. 73–85.

[2]Anderson, J. D., *Hypersonic and High Temperature Gas Dynamics*, 1st ed., McGraw–Hill, New York, 1989, pp. 626–636.

[3]Bird, R. B., Stewartson, W. E., and Lightfoot, E. N., *Transport Phenomena*, 1st ed., Ambrosiana, Milan, Italy, 1960, pp. 518–523 (in Italian).

[4]Baulch, D. L., Drysdale, D. D., Home, D. G., and Lloyds, A. C., *Evaluated Kinetic Data for High Temperature Reactions*, Vol. 2, 1st ed., Butterworths, London, 1973.

[5]Stull, D. R., and Prophet, H., "JANAF Thermo-Chemical Tables," Office of Standard Reference Data, National Bureau of Standards, NSRDS-NBS 37, Washington, DC, June 1971.

[6]Prabhu, R. K., and Erikson, W. D., "A Rapid Method for the Computation of Equilibrium Chemical Composition of Air to 15,000 [K]," NASA TP-2792, March 1988.

[7]Zuppardi, G., Verde, G., and Esposito, A., "Numerical Modeling of an Arc Jet Wind Tunnel," Dipartimento di Scienza ed Ingegneria dello Spazio "Luigi G. Napolitano," Rept. J-96-1, Naples, Italy, Jan. 1996 (in Italian).

[8]De Filippis, F., and Serpico, M., "Air High Enthalpy Stagnation Point Heat Flux Calculation," Centro Italiano Ricerche Aerospaziali, TN-96-014, Capua, Italy, Jan. 1996.

[9]De Filippis, F., Schettino, A., Serpico, M., and Borrelli, S., "Complete Analytical Model to Describe the Test-Leg of Scirocco PWT," *Proceedings of the 20th Congress of the International Council of the Aeronautical Sciences (ICAS-96)*, Sorrento, Italy, 1996, pp. 834–841.

[10]Rose, P. H., and Stark, W. I., "Stagnation Point Heat Transfer Measurements in Dissociated Air," *Journal of the Aeronautical Sciences*, Vol. 25, No. 2, 1958, pp. 86–97.

[11]Rose, P. H., and Stankevics, J. O., "Stagnation-Point Heat Transfer Measurements in Partially Ionized Air," *AIAA Journal*, Vol. 1, No. 12, 1963, pp. 2752–2763.

[12]Horton, T. E., and Babineaux, T. L., "Influence of Atmospheric Composition on Hypersonic Stagnation-Point Convective Heating," *AIAA Journal*, Vol. 5, No. 1, 1967, pp. 36–43.

[13]Yee, L., Bailey, H. E., and Woodward, H. T., "Ballistic Range Measurements of Stagnation-Point Heat Transfer in Air and in Carbon Dioxide at Velocities up to 18,000 Feet per Second," NASA TN-D-777, March 1961.

T. C. Lin
Associate Editor

Flow Visualization on Lower Surfaces of Wave Rider Configurations at Mach 5.5

T. Ohta* and R. Matsuzaki†
Tokyo Metropolitan Institute of Technology, Hino-City, Tokyo 191-0065, Japan

Nomenclature

L/D = lift-to-drag ratio
M_∞ = freestream Mach number
β_s = conical shock-wave angle
δ = one semivertex angle
ε = emissivity

Introduction

SINCE the pioneering work of Nonweiler[1] and Jones,[2] wave riders did not attract researchers' attention for a long time until, in 1980, Rasmussen[3] proposed a cone-derived wave rider. Later, Rasmussen and his co-workers designed an optimized configuration[4] of the cone-derived wave rider. Since then, experimental[5–7] and theoretical[8–13] studies, including design and evaluation based on computational fluid dynamics, have been performed extensively on this configuration. In these configurations, a high-pressure layer below the body is created with a shock wave attached to the leading edge. Hence, the flowfield on the lower surface is of particular importance. Little experimental work has been performed on the nature of the lower-surface flowfield, especially on the surface heat transfer effect. The purpose of the present study is to investigate experimentally the characteristics of the flowfield around such configurations. We observe the flowfields on the lower surfaces of two general cone-derived wave riders, a general cone-derived wave rider (GCWR), and an optimized GCWR using oil-flow, wall-tracing, and infrared thermographic methods. The oil-flow method makes it possible to observe the detailed flow pattern on the lower surfaces whether or not the compressed flow has leaked from the lower compression region through the leading edge. The thermographic measurement is performed to observe the surface temperature fields due to the aerodynamic heating.

GCWR

The GCWR was originally proposed by Rasmussen[3] in 1980 based on the hypersonic small disturbance theory (HSDT). Later such a configuration was numerically tested[9] with the solution of the Euler equation. Stecklein and Hasen[9] designed their configurations based on the Taylor–Maccoll equation "cast in hypersonic small disturbance form." We design the GCWR based on the exact

Received May 7, 1997; presented as Paper 97-1884 at the AIAA 28th Fluid Dynamics Conference, Snowmass Village, CO, June 29–July 2, 1997; revision received Feb. 12, 1998; accepted for publication Feb. 16, 1998.

*Graduate Student, Department of Aerospace Engineering. Student Member AIAA.

†Professor, Department of Aerospace Engineering. Member AIAA.

solution of the Taylor–Maccoll equation[14] without using HSDT assumptions and keeping in mind our low hypersonic test condition ($M_\infty = 5.5$). Figure 1a shows a typical example of our GCWR configuration. A cylindrical upper surface was assumed for convenience of the model support. In this study, $\delta = 19.15$ deg and $\beta_s = 23.5$ deg.

Optimized GCWR

By repeated use of the solution procedure of the Taylor–Maccoll equation, we designed an optimum configuration of GCWR. The optimization was made under the constraint of fixed body length, $M_\infty (= 5.5)$, and $\beta_s (= 23.5$ deg), by obtaining the body shape having maximum L/D. The resulting configuration is shown in Fig. 1b. Again a cylindrical upper surface was employed. This configuration has shown theoretically an L/D improved by about 9% in comparison with its original GCWR.

Wind-Tunnel and Oil-Flow Observations

Experiments were performed in the Tokyo Metropolitan Institute of Technology (TMIT) supersonic wind-tunnel system with $M_\infty = 5.5$, a freestream unit Reynolds number of 4.34×10^6/m, and a maximum duration of steady flow of about 22 s. Other specifications of this wind tunnel are shown in Table 1.

Table 1 Specifications of TMIT supersonic wind tunnel

Type	Blow down
Diameter of nozzle at the exit	120.0 mm
Diameter of nozzle at the throat	18.4 mm
Stagnation pressure	860 kPa
Stagnation temperature	850 K
Maximum mass flow rate	0.3 kg/s
Exhaust	Air ejector

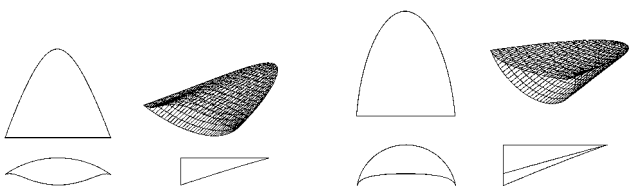

a) Typical example **b) *L/D* optimized**

Fig. 1 GCWR.

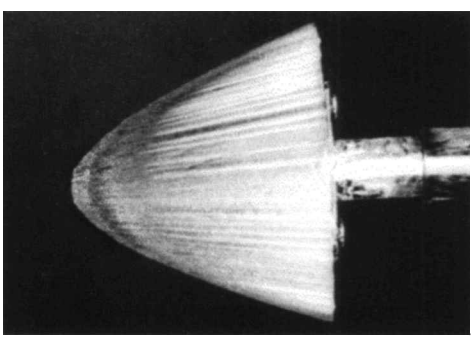

GCWR

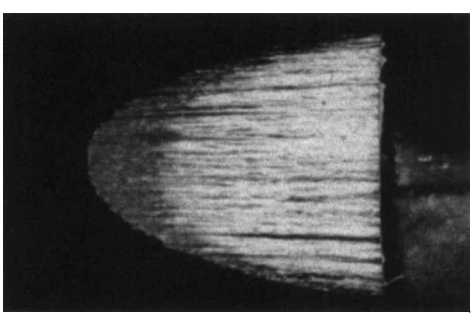

Optimized GCWR

Fig. 2 Oil-flow patterns.

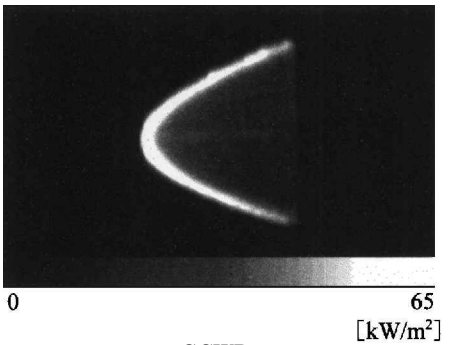

GCWR

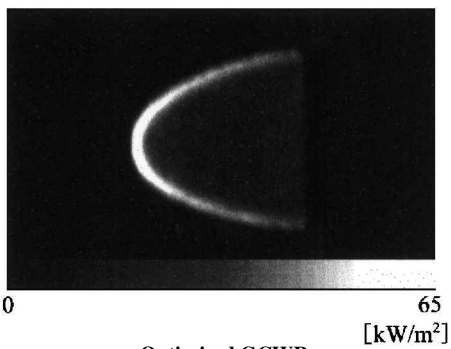

Optimized GCWR

Fig. 3 Heat transfer rate obtained from thermograph.

Both the shape of shock wave and the flow pattern of the lower surface of these wave rider models were observed in a hypersonic flow at Mach 5.5. In particular, flowfields on the lower surface of these models were carefully studied by using an oil-flow observation method. Some examples are shown in Fig. 2. The results show that conical flow is clearly established on the lower surface of the models.

Thermographic Observations

A thermal video system (Japan Avionics, Inc., Type TVS-110) was used. The system was installed inside the test section of the wind tunnel to eliminate the attenuation of radiation through the optical glass window. The radiation from models was detected through a plane mirror. The effect of the mirror was calibrated before the observations. For these observations, models were manufactured using gypsum with $\varepsilon = 0.9$. The value of ε is assumed constant in our temperature range of thermography. An example of the heat transfer rate of the GCWR is shown in Fig. 3. In the experiment, models were cast into the test section using an injection system after a uniform hypersonic flow was established. The heat transfer rate was estimated according to the method of Jones and Hunt.[15]

Conclusions

We have shown that a conical flowfield has been observed on the lower surfaces of GCWRs at Mach 5.5.

Thermographic measurements were performed on the lower surface of the GCWR configuration using gypsum models. Strong aerodynamic heating was observed at the leading edge of the lower surfaces of the wave rider.

References

[1] Nonweiler, T. R. F., "Delta Wing of Shape Amenable to Exact Shock Wave Theory," *Journal of the Royal Aeronautical Society*, Vol. 67, Jan. 1963, pp. 521–528.

[2] Jones, W. P., "A Method for Designing Lifting Configurations for High Supersonic Speeds Using the Flow Fields of Non-Lifting Cones," Royal Aircraft Establishment, Rept. Aero. 2674, March 1963.

[3] Rasmussen, M. L., "Waverider Configurations Derived from Inclined Circular and Elliptic Cones," *Journal of Spacecraft and Rockets*, Vol. 17, No. 6, 1980, pp. 537–545.

[4] Kim, B. S., Rasmussen, M. L., and Jischke, M. C., "Optimization of Waverider Configurations Generated from Axisymmetric Conical Flows," *Journal of Spacecraft and Rockets*, Vol. 20, No. 5, 1983, pp. 461–469.

[5]Rasmussen, M. L., Jischke, M. C., and Daniel, D. C., "Experimental Forces and Moments on Cone-Derived Waveriders for $M_\infty = 3$ to 5," *Journal of Spacecraft and Rockets*, Vol. 19, No. 6, 1982, pp. 592–598.

[6]Jischke, M. C., Rasmussen, M. L., and Daniel, D. C., "Experimental Surface Pressures on Cone-Derived Waverider for $M_\infty = 3$–5," *Journal of Spacecraft and Rockets*, Vol. 20, No. 6, 1983, pp. 539–545.

[7]Hozumi, K., and Watanabe, S., "A Study of Aerodynamic Performance of Cone-Derived Waverider Configurations," *Proceedings of the 1st International Hypersonic Waverider Symposium*, NASA and Dept. of Aerospace Engineering, Univ. of Maryland, College Park, MD, 1990.

[8]He, X., and Rasmussen, M. L., "Computational Analysis of Off-Design Waveriders," *Journal of Aircraft*, Vol. 31, No. 2, 1994, pp. 345–353.

[9]Stecklein, G., and Hasen, G., "Numerical Solution of Inviscid Hypersonic Flow Around a Conically-Derived Waverider," AIAA Paper 93-0320, Jan. 1993.

[10]Takashima, N., and Lewis, M. J., "Navier–Stokes Computation of a Viscous Optimized Waverider," *Journal of Spacecraft and Rockets*, Vol. 31, No. 3, 1994, pp. 383–391.

[11]Eggers, T., Strohmeyer, D., Nickel, H., and Radespiel, R., "Aerodynamic Off-Design Behavior of Integrated Waveriders from Take-Off to Hypersonic Flight," AIAA Paper 95-6091, April 1995.

[12]Lin, S.-C., and Luo, Y.-S., "Integrated Design of Hypersonic Waveriders Including Inlets and Tailfins," *Journal of Spacecraft and Rockets*, Vol. 32, No. 1, 1995, pp. 48–54.

[13]Jones, K. D., Sovieczky, H., Seebass, A. R., and Dougherty, F. C., "Waverider Design for Generalized Shock Geometries," *Journal of Spacecraft and Rockets*, Vol. 32, No. 6, 1995, pp. 957–963.

[14]Rasmussen, M. L., *Hypersonic Flow*, Wiley, New York, 1994, p. 72.

[15]Jones, R. A., and Hunt, J. L., "Use of Fusible Temperature Indicator for Obtaining Quantitative Aerodynamic Heat Transfer Data," NASA TR-R230, Feb. 1966.

J. R. Maus
Associate Editor

Chemical Nonequilibrium Stagnation Ablation Analysis of MUSES-C Superorbital Re-Entry Capsule

Kojiro Suzuki* and Hirotoshi Kubota†
University of Tokyo, Tokyo 113-8656, Japan
and
Kazuhisa Fujita‡ and Takashi Abe§
Institute of Space and Astronautical Science, Kanagawa 229, Japan

Introduction

AT the Institute of Space and Astronautical Science, Japan, the asteroid sample return mission called MUSES-C is in development, aiming for launch in 2002 (Ref. 1). In this mission, a 20-kg small re-entry capsule has the sample container separated from the mother spacecraft on the hyperbolic Earth-return trajectory, and it directly enters the Earth's atmosphere at superorbital velocity to save the spacecraft fuel required for orbital maneuvering. The capsule has an axisymmetric blunt cone configuration with a nose radius Rn of 0.2 m, semiapex angle of 45 deg, and base diameter of 0.4 m. To protect the payload from the severe aerodynamic heating of a superorbital re-entry, use of a carbon–phenolic-type ablator is planned. The peak stagnation aerodynamic heating is expected to occur around 60-km altitude, where the shock layer flow is in full chemical nonequilibrium. Consequently, for evaluation of the heat shield performance, we must consider the chemical nonequilibrium of the freestream and the ablation products through the shock layer, in combination with the finite rate chemical reactions at the ablator surface. The objectives of this study are to present the boundary conditions at the ablating surface for flow computation over the capsule and to make the trajectory-based analysis on the stagnation-point aerodynamic heating environment for the MUSES-C superorbital re-entry capsule by using the viscous shock-layer (VSL) method.

Presented as Paper 97-2481 at the AIAA 32nd Thermophysics Conference, Atlanta, GA, June 23–25, 1997; received July 28, 1997; revision received Feb. 22, 1998; accepted for publication March 6, 1998.

*Associate Professor, Department of Aeronautics and Astronautics, Graduate School of Engineering, 7-3-1 Hongo, Bunkyo. Member AIAA.

†Professor, Department of Aeronautics and Astronautics, Graduate School of Engineering, 7-3-1 Hongo, Bunkyo. Associate Fellow AIAA.

‡Research Associate, Research Division for Space Transportation, 3-1-1 Yoshinodai, Sagamihara. Member AIAA.

§Professor, Research Division for Space Transportation System, 3-1-1 Yoshinodai, Sagamihara. Member AIAA.

Analysis Model

The stagnation streamline equations for the laminar axisymmetric VSL equations with chemical nonequilibrium and thermal equilibrium are solved by the finite difference method. For the freestream and ablation products, we consider 11 air species (N_2, O_2, N, O, NO, NO^+, e^-, N^+, O^+, N_2^+, O_2^+) and 8 carbon-containing species (C, C_2, C_3, CO_2, CO, CN, CO^+, C^+). Details of the present analysis model are given in Ref. 2. The ablating wall is described as the boundary conditions for the VSL analysis in the following way.

The mass fraction of the ith species C_i at the wall is determined by solving the surface mass balance equation written in the generalized form

$$-\rho D_i \cdot \left(\frac{\mathrm{d}C_i}{\mathrm{d}y}\right) + \rho \cdot C_i \cdot v_w = J_i^{\mathrm{cat}} + J_i^{\mathrm{ion}} + J_i^{\mathrm{oxi}} + J_i^{\mathrm{sub}} + J_i^{\mathrm{pyro}} \tag{1}$$

where ρ is the density of gas mixture and D_i is the diffusion coefficient of ith species. The first and the second terms on the left-hand side represent the normal (y-direction) fluxes due to diffusion and ablation injection v_w, respectively. The mass flux due to the catalytic recombination J_i^{cat} is given by the finite catalytic wall model[3]

$$J_i^{\mathrm{cat}} = -\rho \cdot C_i \cdot \gamma_i^{\mathrm{cat}} \sqrt{RT_w/2\pi M_i} \qquad (i = \mathrm{N}, \mathrm{O})$$
$$J_{\mathrm{N}_2}^{\mathrm{cat}} = -J_{\mathrm{N}}^{\mathrm{cat}}, \qquad J_{\mathrm{O}_2}^{\mathrm{cat}} = -J_{\mathrm{O}}^{\mathrm{cat}}, \qquad J_i^{\mathrm{cat}} = 0 \qquad (i = \text{others}) \tag{2}$$

where T_w is the wall temperature, M_i is the molecular weight, and γ_i^{cat} is the reaction probability for the catalytic recombination. The noncatalytic wall (NCW) and the fully catalytic wall (FCW) are described as $\gamma_i^{\mathrm{cat}} = 0$ and $\gamma_i^{\mathrm{cat}} = 1$, respectively. The mass flux due to recombination of ions and electron J_i^{ion} is given in the same way.

The thermochemical properties of the ablator surface are expected to be similar to those of graphite because the surface of the carbon-phenolic ablator becomes a char layer of carbon under the severe aerodynamic heating of superorbital re-entry. Two types of reactions involving phase change at the surface, that is, oxidation by atomic oxygen and sublimation into the C_3 molecule, are considered. The mass flux due to the surface oxidation by atomic oxygen J_i^{oxi} is presented as[4]

$$J_i^{\mathrm{oxi}} = -\rho \cdot C_i \cdot \gamma_i^{\mathrm{oxi}} \sqrt{RT_w/2\pi M_i} \qquad (i = \mathrm{O})$$
$$J_{\mathrm{CO}}^{\mathrm{oxi}} = -J_{\mathrm{O}}^{\mathrm{oxi}} \cdot (M_{\mathrm{CO}}/M_{\mathrm{O}}), \qquad J_i^{\mathrm{oxi}} = 0 \qquad (i = \text{others}) \tag{3}$$

where γ_i^{oxi} is the reaction probability for the reaction $\mathrm{C}(s) + \mathrm{O} \rightarrow \mathrm{CO}$. Note that the constraint $\gamma_{\mathrm{O}}^{\mathrm{cat}} + \gamma_{\mathrm{O}}^{\mathrm{oxi}} \leq 1$ exists because the mass flux $-J_{\mathrm{O}}^{\mathrm{cat}} - J_{\mathrm{O}}^{\mathrm{oxi}}$ never exceeds the mass flux of the atomic oxygen striking the wall. The surface mass flux due to sublimation is given by the Hertz–Knudsen–Langmuir relation[4]

$$J_i^{\mathrm{sub}} = \alpha_i \cdot (p_{e,i} - p_i)/\sqrt{2\pi(R/M_i)T_w} \qquad (i = \mathrm{C}_3)$$
$$J_i^{\mathrm{sub}} = 0 \qquad (i = \text{others}) \tag{4}$$